光学学报

基于成像光电容积描记技术的非接触式生理参数检测及其应用

孔令琴[1,2,3]，赵跃进[1,2,3*]，董立泉[1,2,3]，刘明[1,2,3]，徐歌[1]，惠梅[1]，褚旭红[1,2,3]

[1]北京理工大学光电学院，北京 100081；

[2]精密光电测试仪器与技术北京市重点实验室，北京 100081；

[3]北京理工大学长三角研究院，浙江 嘉兴 314019

摘要 成像式光电容积描记技术是在传统光电容积描记技术基础上发展而来的一种非接触式生理信号检测技术。成像式光电容积描记技术由于非接触、可远程监测、适用场景广泛、易操作以及低成本等优点可实现人体多项生理参数的测量，成为仪器及生物医学工程领域的新兴研究热点之一。本综述首先介绍了成像式光电容积描记技术的基本原理，对光学起源机理进行了分析，并对成像视频处理方法进行了总结，最后介绍了成像式光电容积描记技术在生理参数方面的应用，并对其在生理参数检测领域中的发展进行展望。

关键词 成像式光电容积描记技术；生理参数检测；心血管监测

中图分类号 Q632 **文献标志码** A **DOI**：10.3788/AOS230755

1 引 言

成像式光电容积描记(IPPG)[1]技术是在传统单点光电容积描记(PPG)[2-3]技术的基础上，利用成像设备将光与皮肤组织内部发生相互作用后携带心脏脉动信息的漫反射光所引起的皮肤颜色的微小变化以连续图像的形式记录下来，并通过视频分析和图像处理技术，从视频流中提取出人体生命体征信息如脉搏、心率、心率变异性等的一种非接触、无创生理参数检测技术。

IPPG技术克服传统接触式PPG技术存在的接触式操作应用场景受限、接触力导致生理参数测量精度低以及受人体佩戴方式干扰等问题，以非接触、可远程监测、性价比高、设备操作过程简单以及能够对受试者进行连续自动测量观察的优点，在人体生理参数检测应用上取得了长足进展。目前IPPG技术已经从心率、呼吸率以及心率变异性[4-8]等基础生命体征参数检测逐渐过渡到对复杂疾病如动脉疾病、僵硬和老化等慢性微循环疾病[9-11]的监测。IPPG技术有望成为深入理解生物组织的光学特性和探究复杂心血管疾病相关病理机理的重要手段。

慢性病症状通常会使得人体呈现“亚健康”状态，即心率、心电、血压以及血氧饱和度等基础生命体征参数发生变化。通过对上述参数进行实时监测，就能在慢性病早期做到提前发现，并采取及时治疗等措施避免其进一步恶化。IPPG技术揭示生物组织在生理与病理过程中发生的动态、微小改变，成为了研究重要疾病(特别是早期病变)的新思路和新手段。IPPG技术适用于大规模临床检测及日常生活中身体健康状况监测等场景，是医疗健康新时代下的人体日常生理状态监测的研究热点。本文在综合调研近20年来国内外采用IPPG技术进行人体生理参数监测的大量相关文献基础上，结合本研究团队在该领域所开展的研究工作，从IPPG技术的生理学机理着手，探究IPPG技术的光学起源机理，分析IPPG信号处理方法，最后，根据本研究团队的工作内容介绍IPPG技术的应用及发展情况。

2 IPPG技术基本原理

2.1 PPG技术

PPG技术是获取脉搏波的重要手段，通常以受试者手指、手臂或面部作为被检测部位提取脉搏波信号即PPG信号。PPG技术按传感器接收光的方式可分为透射式和反射式两种，如图1所示。在透射式中，光源与光电传感器分别位于被检测部位相对应的两侧，从光源发出的光穿过被检测部位进入深层组织，除被

收稿日期：2023-03-30；**修回日期**：2023-04-27；**录用日期**：2023-05-06；**网络首发日期**：2023-05-16

基金项目：国家自然科学基金(61705010，11774031，61935001)

通信作者：*yjzhao@bit.edu.cn

皮肤中的生色团、血液等吸收外，一部分由血液漫反射回来，其余部分则透射出去。透射式适用于指尖、耳垂、脚趾等较薄的身体部位。传统脉搏血氧仪采用的就是透射式PPG技术，可以测量人的血氧饱和度和心率水平。

对于反射式PPG来说，光源和光电传感器件位于被检测部位同侧，光电传感器接收被组织反射回来的漫反射光。反射式PPG理论上可以应用在人体任何裸露的皮肤组织表面。目前广泛流行的能够实现血氧饱和度、心率等生理参数测量的智能手环等商业产品采用的是反射式PPG技术。

接触式PPG传感器的使用受到一定的限制，接触式测量方式需要与被测者产生肢体接触，对于一些危急情况如烧伤、创伤、严重感染等，佩戴接触式设备存在极大的不便性。此外，接触式方式会对使用者产生心理压力，从而影响心血管生理参数的测量精度。

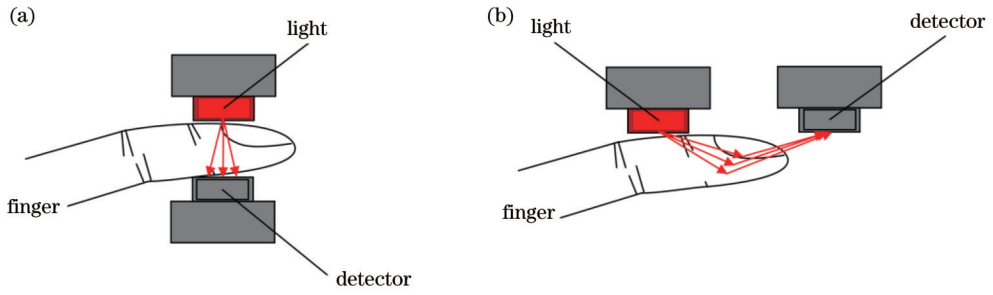

图1 PPG技术。(a)透射式PPG技术；(b)反射式PPG技术

Fig. 1 PPG technology. (a) Transmission model of PPG technology; (b) reflection model of PPG technology

2.2 IPPG技术

IPPG技术是在反射式PPG技术的基础上发展而来的。IPPG系统通常由光源、皮肤组织以及图像传感器等3部分组成。图2为漫反射IPPG技术的物理模型。光源发出的光一部分透过皮肤表皮进入组织内部，在皮肤组织内部发生散射、反射以及吸收等光学作用，另一部分在皮肤表面发生镜面反射。图像传感器接收到的光信号包含与皮肤组织内部发生相互作用后携带心脏脉动信息的漫反射光以及直接从皮肤表面反射回去的没有携带生理信息的镜面反射光。

由于心脏搏动产生的振动会随血管组织传至人体外周微血管及皮肤组织，微弱的振动会引起皮肤组织光吸收量的变化即人体血管中的血液容积变化。血红蛋白对光具有一定的吸收作用，真皮层血容量周期性变化使其对光的吸收也发生周期性调制，进而导致皮肤表层的微弱颜色变化。肉眼虽然无法观察到这样的周期性变化，但却能够被成像传感器所捕捉。因此，光穿过皮肤表层后的衰减特性以光学连续图像的载体形式呈现，通过图像处理技术处理后可得到心率、心率变异性以及血氧饱和度等生命体征。

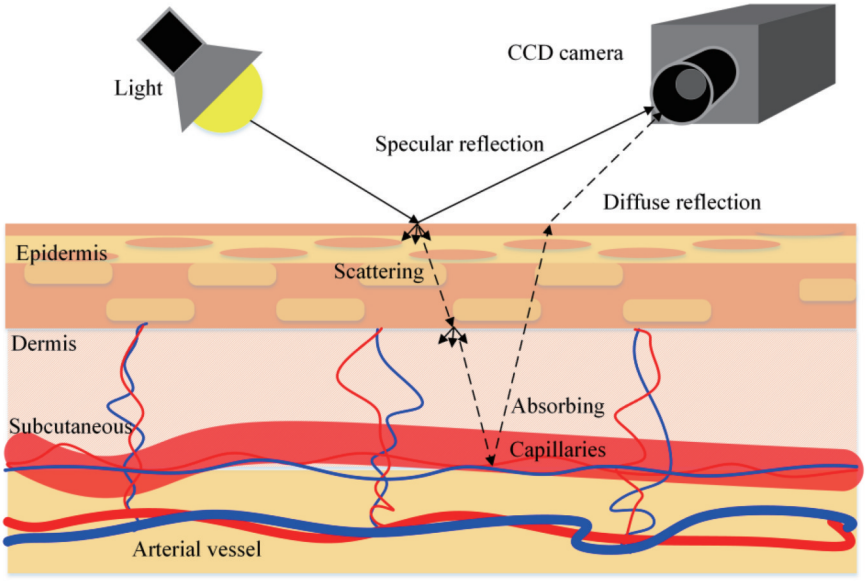

图2 反射式IPPG技术

Fig. 2 Reflection model of IPPG technology

测得的IPPG波形包括一个脉动(AC)生理波形以及大趋势缓慢变化的准静态(DC)基线。AC波形反映每次心跳时血液体积的心脏同步变化,DC成分则包含呼吸、静脉流量、交感神经系统活动和体温调节信息。很多研究人员已经对IPPG信号的波形特点进行了理论方面的深入研究[9],故在此不详细阐述这部分内容。

2.3 IPPG技术光学起源机理

2008年,Verkruysse等[12]首次采用白光作为IPPG技术的光源。目前以白光作为IPPG技术的光源已经得到了普遍认可[13-15]。白光作为IPPG技术的光源时,成像传感器RGB三通道中都均能获取携带脉搏信息的IPPG信号,且绿色通道IPPG信号脉动幅度远远大于红、蓝通道,这与传统PPG技术主要收集来自与动脉血管交互的光信号[16]相矛盾。事实上,由于绿光的透射深度小于1 mm,一般只与毛细血管交互,无法到达位于3 mm以下的深层动脉及小动脉,这使得IPPG技术的光学起源机理出现了争议。针对IPPG技术的光学起源机理,目前产生了3种主流观点:

1)动脉血液流入毛细血管时,对毛细血管壁产生压力,导致毛细血管直径周期性变化,因此毛细血管的血容积变化对到达真皮层的绿光进行了直接周期性调制[17-19]。

心脏周期性跳动时,动脉血液涌入毛细血管会对其血管壁产生压力,导致毛细血管直径发生周期性变化。毛细血管直径的周期性变化又会导致其血容积的变化,从而对到达真皮层的绿光进行了周期性调制而产生了IPPG信号。RGB三通道IPPG信号中绿通道的IPPG信号具有最高的信噪比[20]。这是由于常规图像传感器在RGB某一通道测得的IPPG信号是血液在该图像传感器通道波段的吸收系数、光谱响应情况及光源穿透皮肤组织深度所共同决定的。

血液中的血红蛋白以及含氧血红蛋白对蓝光的吸收系数最大,绿光次之,红光最小,如图3(a)所示。而蓝光的透射深度最小,绿光次之,红光最大,如图3(b)所示。同时常规成像传感器在绿光处响应最高,蓝光与红光次之。因此,虽然三波段中红光穿透深度最深,能够与深层动脉血发生交互,但常规成像传感器在该波段的响应及血液对其吸收并不高。换言之,虽然成像传感器在蓝光波段有较强的响应,但蓝光在皮肤的穿透深度最浅。因此最终绿光信号能更好地携带心脏的搏动性信息,交流脉动分量更大,如图3(c)所示。

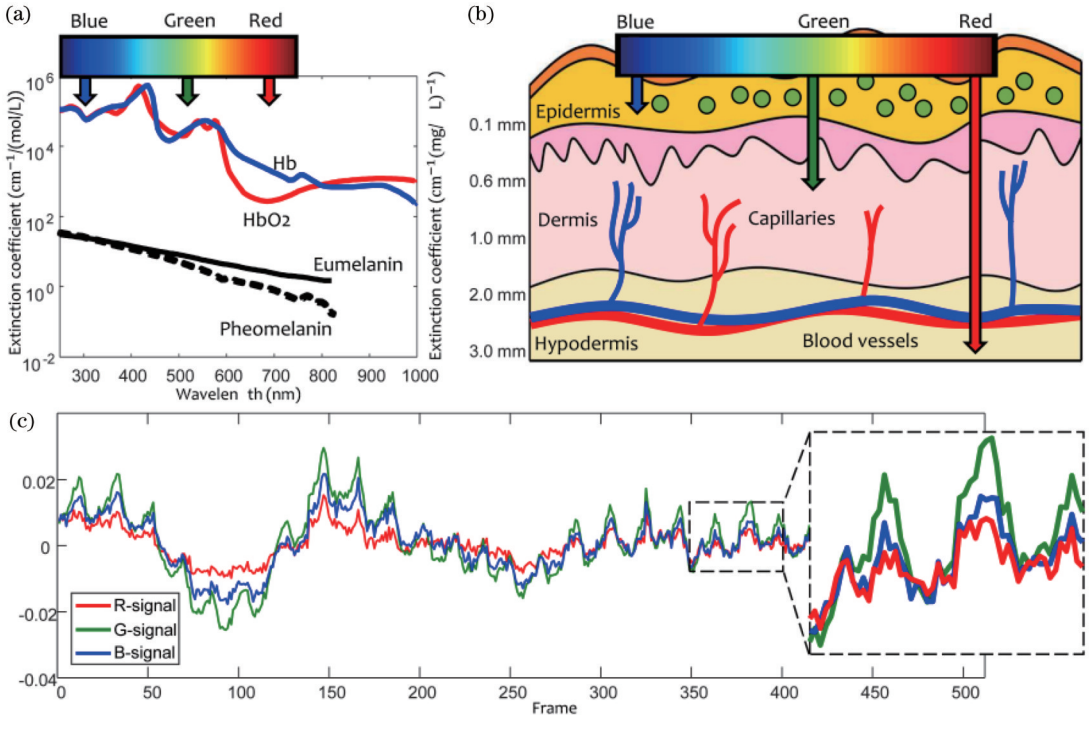

图3 血液成分与光穿透深度[20]。(a)血红蛋白对红绿蓝三色光的吸收程度;(b)红绿蓝三色光在皮肤中的透过深度;(c)红绿蓝通道信号的调制幅度

Fig. 3 Blood composition and light penetration depth[20]. (a) Absorption of red, green and blue light by hemoglobin; (b) penetration depths of red, green and blue light in the skin; (c) modulation amplitudes of red, green and blue channels

但是后续对毛细血管力学性能的研究表明,随着心脏跳动,毛细血管的直径几乎没有变化,血容量的变化也主要发生在动脉和小动脉中。因此,毛细血管直径周期性变化导致其血容积变化,进而对到达真皮层的绿光周期性调制产生IPPG信号的说法也似乎并不成立。

2)毛细血管内红细胞速度信号相位变化导致光信号的周期性调制[21-23]。

毛细血管血液流速是变化的,根据流体力学可知,毛细血管血液流速的变化会导致血液与红细胞膜间发生相对位移,二者产生的内摩擦力使得红细胞的横截面积发生改变。红细胞变形过程中,血液中红细胞的各向异性的角度发生变化,即与光作用的红细胞的横截面积发生变化。因此,红细胞横截面积的改变会导致光的吸收与散射系数发生变化,从而导致IPPG信号波形的产生。

但有实验研究表明[24],采用绿光照射手指皮肤并对其施加一定压力时,从该处皮肤得到的IPPG信号的AC成分的振幅与无压力时相比有显著提高。该现象无法用毛细血管内红细胞流速信号的相位变化来解释,IPPG信号产生机理再次受到质疑。

3)真皮毛细血管床的血容量密度变化影响光的吸收和散射系数,进而产生IPPG信号[13-14, 25],如图4所示。

血压力导致动脉直径周期性振荡,并对与其相邻的毛细血管床产生周期性挤压,导致毛细血管床发生周期性弹性形变。毛细血管床周期性弹性形变调节了毛细血管床密度,使得毛细血管之间的距离发生变化,局部区域整体血容量发生周期性变化,最终导致组织光吸收和散射量发生周期性变化。

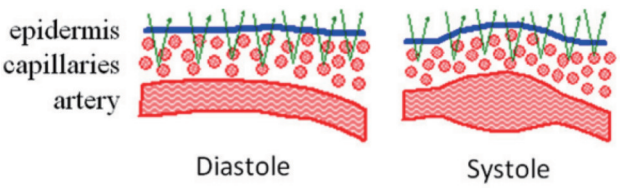

图4 IPPG波形起源[13]

Fig. 4 Origin of IPPG waveform[13]

由于心脏搏动产生的振动会随动脉传播。考虑到真皮层的力学性能,动脉血管壁的振动会导致与其相邻的毛细血管床发生周期性弹性形变,这种周期性形变调节了真皮毛细血管床的血容量,改变了毛细血管血容量密度,从而影响了光的吸收和散射,进而产生了IPPG信号。

IPPG技术的光学起源机理还有待进一步的实验验证,很多研究人员也仍然在IPPG的光学起源机理上进行不断深入的研究。

2.4 IPPG信号预处理方法

IPPG技术信号的处理流程如图5所示,主要包含3个过程:从原始包含皮肤组织的视频中获得检测部位的时序图像、从连续多帧时序图像中提取RGB三通道IPPG信号、根据RGB三通道IPPG信号计算相应的生理参数信息。

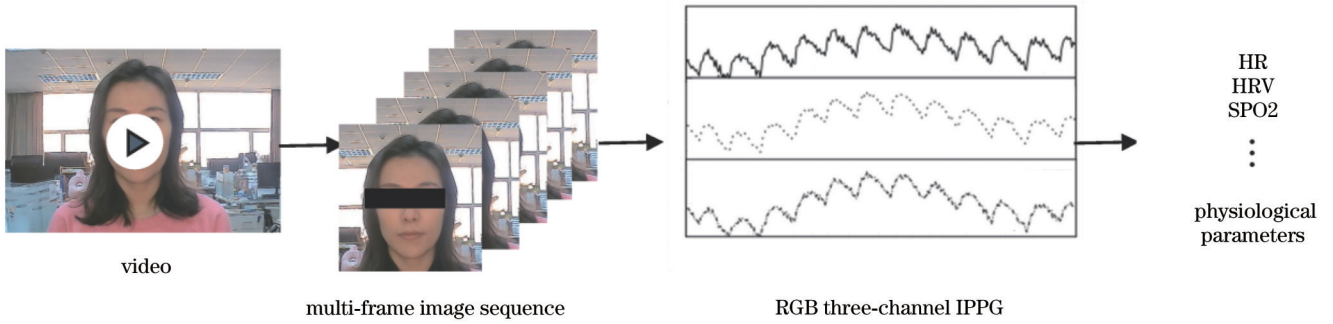

图5 IPPG技术生理参数获取流程图

Fig. 5 Flow chart of physiological parameter acquisition of IPPG technology

2.4.1 视频处理

一般来说,人体皮肤组织视频图像中均能够提取出IPPG信号。但在实际应用中,主要采集血液灌注相对丰富、色素沉积少且便于成像设备拍摄的人体部位。因此,手指、手臂以及面部是主要的IPPG信号获取区域。

IPPG技术中常用的人脸检测方法主要有人脸检测器Viola-Jones(VJ)算法[26-28]、进行面部特征点的检测与跟踪的约束局部神经域(CLNF)算法[29-30]以及利用核检测跟踪的循环结构(CSK)算法[31]等。VJ人脸检测器算法能够进行面部感兴趣区域的自动选择,通过检测视频帧内的人脸定位每个视频帧的感兴趣区域。该算法主要用于正面面部样本的训练,当面部位置偏离正面位置时,会导致后续视频帧中出现不连续的面部定位。人脸跟踪[32]是针对人体存在运动伪影的情况下进行面部区域IPPG信号提取的算法。在VJ算法的基础上融入皮肤检测[33-34]可以进一步提高感兴趣区域的定位精度。超体素分割与字典学习结合的活体皮肤检测voxel pulse spectral(VPS)算法[35]能够保留皮肤区域的轮廓信息,克服皮肤区域无法精确分割的问题。但VPS算法在分割图像时,计算过于复杂且计算量大,不能实时检测视频中的活体皮肤。随后,Wang等[36]改进了VPS算法,提出一种基于多分辨率光谱迭代的实时活体皮肤检测算法,将时变IPPG信号转换为多分辨率迭代频谱进行分类训练,提高了实时性。

将视频图像分割成多个子区域，通过对多个子区域开展心率评估的方法也得到了进一步发展。Liu等[37]提出一种基于IPPG心率信息的人脸皮肤检测算法。首先，将视频图像分割成多个40 pixel×30 pixel大小的子区域，并计算出每个子区域的心率信息。然后，以受试者额头区域的心率为参考心率，通过比较每一块子区域的心率信息与参考心率之间的差异来实现人脸皮肤与非皮肤区域的分离和判断。Tarassenko等[38]利用Kanade-Lucas-Tomasi(KLT)方法实现人脸追踪，通过非参数贝叶斯图像分割获得人脸准确位置，然后从脸颊或者额头上选取100 pixel×100 pixel的感兴趣区域从而实现心率检测。

手臂、手掌的肤色分布均匀，皮肤表面相对平整且血液灌注充盈，因此主要使用阈值分割方法[39]、高斯肤色模型[40]等对上述部位进行IPPG信号提取。

2.4.2 滤波以及去基线漂移

由于成像设备的拍摄区域往往包含无规则背景，且检测部位的成像大小与角度也会随人体晃动而发生变化。因此，常采用如下技术手段对IPPG信号进行处理，以提高IPPG信号信噪比。

基于盲源分离(BSS)的IPPG提取算法[41-42]将时域RGB三通道颜色信息解耦到不相关或相互独立的信号源中，以检索IPPG脉搏波信号。基于正交肤色平面(POS)的IPPG算法[43-45]以皮肤像素子空间的色相变化表示IPPG脉搏波信号。色度(CHROM)方法[46-49]利用不同颜色通道对血液脉动的不同吸收特性来设计投影函数，并将原始RGB信号投影到该函数方向上，从而分离出IPPG脉搏波信号。

提取IPPG信号后则采用颜色失真滤波(CDF)算法[50]、先验平滑滤波[51]以及小波滤波[52]等进一步对脉搏波信号进行去趋势处理，得到高信噪比的IPPG信号。表1对不同IPPG信号处理方法进行了总结。

实际上，大部分IPPG信号滤波方法主要用来提升心率计算的准确性，虽然过度滤波在一定程度提升了心率的准确性，但易损失脉搏波波形上所反映的血管壁细节特征[55-57]以及血液黏稠度信息。Yu等[58]通过滤波器组方法提取的IPPG信号波形接近正弦波，但滤波后的波形上重搏波缺失。Kumar等[59]使用加权平均值方法来提取面部不同区域的肤色变化信号，其中，加权平均值的权重取决于该区域内血液灌注情况以及入射光强度。该IPPG信号获取方法具有良好的抗噪性能，但IPPG信号波形上仍然看不到明显的重搏波。Wang等[60]提出自适应奇异频谱分析算法以获得IPPG信号周期成分并去除非周期不规则噪声。采用该算法从面部视频中提取的脉搏波在细节保留和实时心率估计方面优于现有技术，并且能够作为心房颤动、心率变异性、血压以及其他生理指标的标准脉搏波，但其复杂度较高。

表1 IPPG信号的不同处理方法以及优缺点

Table 1 Different processing methods of IPPG signal and its advantages and disadvantages

Method	Advantage/disadvantage
CDF	In the frequency range, the IPPG signals of R, G and B channels are weighted with different weights, which effectively suppresses the color distortion caused by motion
POS	HR is accurately measured at rest or with light movement
BSS	BSS method is superior to ICA method
CHROM	CHROM method is better than ICA method in motion
Wavelet	IPPG signals can be separated from facial video data during motion
ICA[53-54]	Steady heart rate extraction when the subject is near and at rest

由于IPPG信号本身含有丰富的生理参数信息，因此针对IPPG技术采取何种滤波方法与需要提取的生理参数密切相关。

3 IPPG技术的应用

IPPG技术应用领域十分广泛，以下重点结合北京理工大学光电学院在该领域内的研究进行介绍。

3.1 心率

心率(HR)和心率变异性(HRV)的提取方法主要分为时域法和频域法。时域法从脉搏波时域信号中提取出脉搏波的峰值点或谷值点，计算相邻特征点之间的时间差值从而求得受试者的每一次心跳周期，即心率值。IPPG信号中除了脉搏波还包含有其他生理信号及噪声信号，由于脉搏波信号和其他信号在各个频率段的功率分布不同，频域内心率计算方法采用傅里叶变换(FFT)将IPPG信号从时域转换至频域[61-62]，并通过频谱分析估算出心率值。频域内幅值最大处的频率值为心率值，频率法也是常用的心率算法。

提高远距离心率准确性测量的前提是提高IPPG信号信噪比。针对远距离运动下需克服受试者与成像设备间的物距迅速变化所引起的图像中敏感区域大小、特征灰度剧烈变化等问题，Kong等[63]提出并设计了一种自适应焦距下的IPPG心率监测系统(AZIPPG)，该系统可以抑制敏感区域的剧烈变化，有效降低其对IPPG信号的干扰，并从理论和实验上证明了IPPG信号的提取对离焦模糊不敏感，实现了远距离步行状态下心率的准确检测。

AZIPPG系统在远距离步行运动过程中基于模糊

图像提取到的IPPG信号与传统BVP设备所采集到的PPG信号的对比分析表明：从模糊图像中提取的IPPG信号与接触式BVP脉搏波传感器提取的PPG信号有着相同特点，两者峰值一一对应且具有良好的一致性，如图6(a)所示；此外，两种方法提取到的脉冲信号是具有一定的相位差的，这是两种方法检测位置不同引起的。两种方法的Pearson相关系数均为0.8005，如图6(b)所示。使用Bland-Altman分析来评估AZIPPG和BVP设备之间的心率一致性，如图6(c)所示，其中，Bland-Altman的下限和上限分别为−6.79 BPM和7.43 BPM，且所有测量心率数据值均在95%置信区间内，两者具有较高的一致性，BMP为每分钟心脏跳动次数。

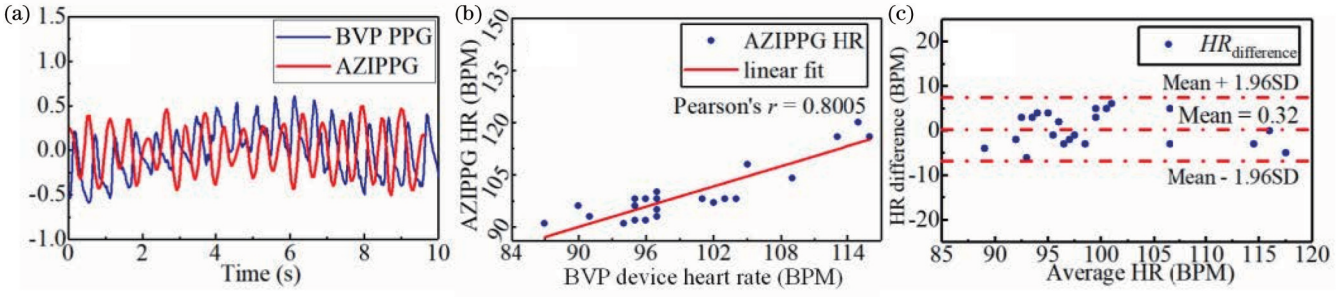

图6 AZIPPG运动实验测量结果[63]。(a)脉搏波信号对比图；(b) Pearson相关系数；(c) Bland-Altman分析

Fig. 6 Measurement results of AZIPPG motion experiment[63]. (a) Comparison of pulse wave signals; (b) Pearson correlation coefficient; (c) Bland-Altman analysis

3.2 活体皮肤检测

IPPG活体皮肤检测利用深层的生理参数信息作为判断依据，可区分视频图像中活体皮肤组织和类皮肤模型，在身份识别、面部防骗、手势表情识别等领域扮演着非常重要的角色[64-66]。不同人种的肤色差异、有色光源照射、成像设备色偏以及待测者处于复杂光照情况下时，活体皮肤在图像中的表象会更加复杂多变，使得通过IPPG技术实现视频图像中活体皮肤的精确检测变得更加复杂，具有挑战性[67]。

超像素(子区域)是由一系列位置相邻且具有相似纹理、亮度等特征的像素点组成的不规则小区域[68]。作为活体皮肤检测的第一步，超像素分割效果影响活体皮肤检测效果和生理参数提取的准确性。常规聚类分割算法如分水岭算法、K均值(K-mean)聚类算法等对比度明显的人体皮肤图像有较好的分割效果。基于谱聚类超像素分割算法[69-70]通过不同的权值使各超像素面积大小相似，能够提升活体皮肤检测的效果。Vedaldi等[71]提出一种利用均值平移、自底向上的超像素生成算法来提升谱聚类生成速度。Achanta等[72-73]提出简单线性迭代聚类(SLIC)算法。SLIC算法是在一个由CIELAB颜色空间的L、A以及B结合位置坐标X、Y所构成的5维特征空间中依靠特定距离度量标准进行的局部像素点聚合过程。SLIC算法所需参数较少且生成的各个超像素子块排列紧凑、大小均匀，同时较好地保留了图像中物体的轮廓边界等细节信息，使得子区域块有着较好完整性。

针对现有活体皮肤检测方法精度不高、实时性较差的问题，孔令琴等[74]设计并提出了一种超像素-活体皮肤检测(SPASD)算法。首先，利用零参数简单线性迭代聚类算法将图像分割为多个超像素子块；然后，通过IPPG技术并行提取各子块中的脉搏波信号；最后，利用支持向量机对提取到的信号进行训练分类，进而实现活体皮肤的实时检测。SPASD算法利用改进的SLIC算法实现了对活体皮肤的精确快速分割，有效提高了系统检测精度。SPASD算法并行分割处理各超像素子块，提高了实时性。SPASD算法增强了IPPG信号鲁棒性且无需反复迭代，简化了算法复杂度。SPASD算法实现了活体皮肤的精确检测，活体皮肤区域被检测、分离、标记出来，具体如图7(a)～(c)所示。皮肤模型没有被标记，如图7(d)～(f)所示。同时，SPASD算法较好地保留了视频图像中活体皮肤与皮肤模型的轮廓信息，如图7(b)、(e)所示。

3.3 血氧饱和度

血氧饱和度(SPO2)[75-76]能有效反映人体呼吸系统和循环系统的生理状态，在健康监护与病情诊断中发挥着积极作用。心脏舒张和收缩时，人体血液会随着心脏的脉动流经过肺部。血液中脱氧血红蛋白与肺泡中的氧气结合，成为含氧血红蛋白。含氧血红蛋白进入人体后通过毛细血管组织释放氧气，从而促进人体组织细胞的新陈代谢。目前，血氧饱和度也是新型冠状病毒感染重要的诊断指标之一[77]。

常规脉搏血氧计选择两种不同的波长(通常为660 nm和940 nm)的光作为光源，以手指作为检测部位，测量两束光束通过手指后的最大透射或反射强度实现血氧饱和度的测量。两个波长需要具有穿透皮肤深度的能力，能够到达动脉血液，从而使获得的IPPG信号具有高信噪比。同时，两个波长应处于含氧血红蛋白与脱氧血红蛋白吸收差异的最大处。研究人员已

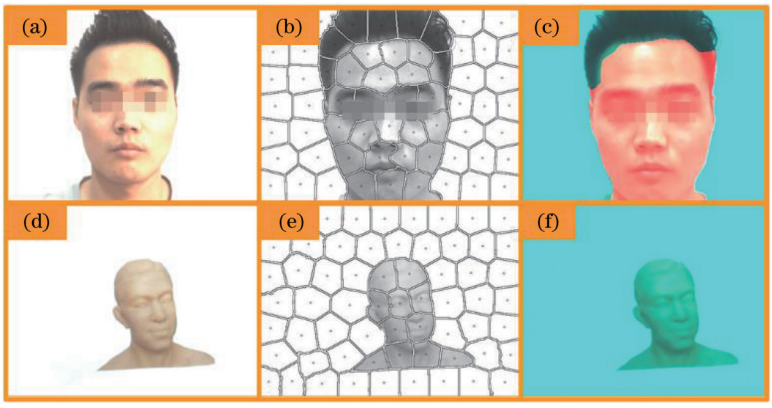

图 7 SPASD 检测结果[74]。(a) 活体皮肤原图;(b) 活体皮肤超像素分割图;(c)活体皮肤检测效果图;(d) 皮肤模型原图;(e)皮肤模型超像素分割图;(f) 皮肤模型检测效果图

Fig. 7 SPASD results[74]. (a) Original live skin. (b) superpixel segmentation map of the live skin; (c) test result of live skin; (d) original skin model; (e) superpixel segmentation map of the skin model; (f) test result of skin model

经探索了如何利用单个成像设备实现双波长下 SPO2 的提取[78-79]。目前基于面部、手指、前臂和手掌等部位实现非接触式 SPO2 测量的研究也很广泛[80-82]。在大多数报道的工作中[83-86],光源的选择主要包括 450~1000 nm 的可见光和近红外光。当涉及近红外光源时,相机传感器需要覆盖近红外光谱范围。环境光下仅使用 RGB 相机进行 SPO2 的监测目前被验证也是可行的[87-88]。

在不外加主动光源的情况下,Kong 等[89]采用加有窄带滤光片的双 CCD 作为视频采集单元,在低照度 CCD 实现环境光下的血氧饱和度的测量。在相同环境温度和光照条件下,对多名志愿者进行多组屏气对比实验后,使用 30 组不同志愿者的 30 组数据对血氧饱和度的经验系数进行校准,从而得到血氧饱和度。血氧饱和度的测量结果如图 8 所示。从图 8 中阴影部分可以看出,非接触器件测量到的 SPO2 值与手指血液容积脉搏波传感器检测到的 SPO2 有很好的线性关系。然而,非接触式设备在 28 s 后的测量结果高于血液容积脉搏波传感器。这是因为在这个时间点之后,受试者已经开始呼吸,而血液饱和度仍在下降,由于人脸血氧饱和度恢复速度比手快,因此导致 28 s 后出现偏差。

3.4 疲劳状态监测

当驾驶员处于疲劳状态时,其生理反应会变慢,身体对刺激的反应出现延迟,进而导致生理指标失调[90]。因此,生理参数传感器采集到的脑电、肌电、心电、脉搏以及呼吸频率等生理信号可以用来判断驾驶员是否处于疲劳驾驶状态。驾驶疲劳检测方法中,基于生理参数[91]判断疲劳状态相较于基于车辆行驶特征方法[90-94]、基于驾驶员行为特征[95-99]方法具有更高的准确率。

睡眠不足的受试者的心电图和脑电图中低频与高频分量的比值较低,很大概率发生交通事故。因此,

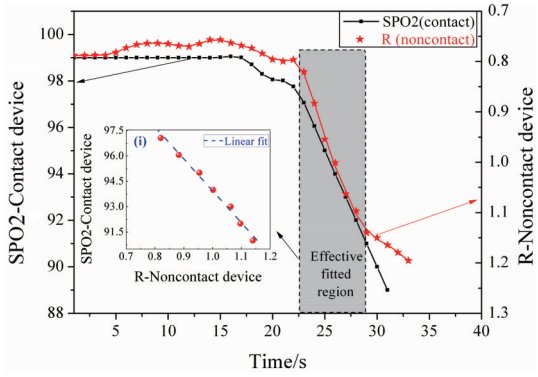

图 8 采用接触式测量仪与提出的非接触式测量方法测量的 SPO2 相关系数 R 值在时间上的比较[89]

Fig. 8 Comparison of the R measured by noncontact device proposed and the SPO2 measured by contact device versus time[89]

HR 和 HRV 指数是反映人体疲惫程度的关键参数,与驾驶警觉状态相关[100-106]。Abe 等[107]提出一种基于自主神经功能来预测疲劳驾驶事故的方法。自主神经功能会影响心率变异性,通过 HRV 特征作为异常检测方法多元统计过程控制(MSPC)的输入变量而开展模拟驾驶实验。实验结果表明,在疲劳驾驶事故发生之前,87.5% 驾驶员被成功预测为疲劳状态。Michail 等[108]证明了对驾驶员的心率功率谱分析可以判断由困倦所引起的驾驶失误。但通过驾驶员佩戴相关仪器获取心电进行疲劳状态的监测方式存在操作繁琐、佩戴物品易影响驾驶员心理压力导致测量结果存在误差等因素。Jung 等[109]通过安装在方向盘上的传感器实时采集驾驶员脉搏信号参数,并对脉搏信号参数进行算法建模分析,实现驾驶员的疲劳程度判断。Shin 等[110]也针对驾驶环境下的心率开展监测,基于摄像头监控系统在后台运行,通过评估驾驶员的生命体征来间接估计驾驶员的压力水平。

在深入分析目前国内外在疲劳驾驶检测及预警方

面的研究基础上，结合生理参数检测及行为特征检测方法的优点，开发了一套基于人脸视频的非接触式双模态疲劳驾驶检测系统。基于IPPG技术的非接触性、可靠性以及预警性等优点，结合驾驶员行为状态检测技术，构建双模态的非接触式疲劳驾驶检测系统。疲劳驾驶检测界面分为视频图像显示窗口、疲劳状态显示窗口和参数显示窗口等。视频图像显示窗口负责实时显示相机采集的图像。疲劳状态显示窗口负责显示疲劳判断决策模型输出的结果，每5 min更新一次。参数显示窗口显示驾驶员的头部姿态角度、心率值等参数。在用户点击开始后开始测量驾驶员的双模态特征，实时显示驾驶员的心率值和头部姿态，满足5 min的时间长度后显示驾驶员的疲劳判断结果。非接触式疲劳驾驶检测系统界面系统示意图如图9所示。

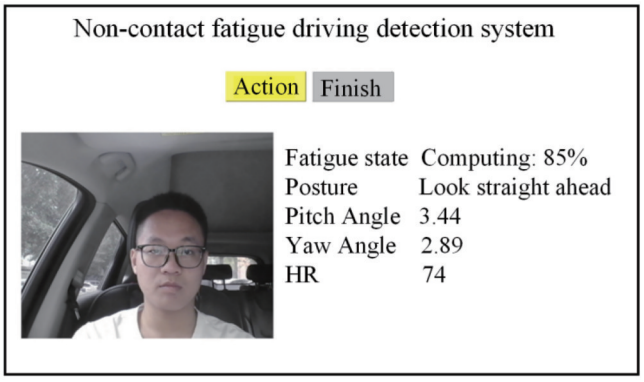

图9 非接触式疲劳驾驶检测系统界面示意图

Fig. 9 Interface diagram of non-contact fatigue driving detection system

3.5 心理压力状态评估

传统心理压力评估方法主要是基于压力量表的主观评估法[111-114]，对心理压力的量化依赖于个体的自我判断与主观经验，难以客观反映被测试者真实的心理状态，且压力评估结果取决于被测试者对待测试的态度，故意隐瞒真实感受、刻意迎合测试期望等情况均会影响测试结果的准确性。

基于生理参数来进行心理压力评估的方法因其没有主观因素的影响而具备更加准确的结果，基于传感器等穿戴式设备测量心率、呼吸率、皮肤电导率等综合生理信息进行心理压力的评估得到学者们的认可[115-116]。然而，传感器等穿戴式设备在使用中佩戴步骤繁琐，限制了其应用。IPPG技术非接触式测量生理参数的优势在心理压力测量中得到了体现。HRV功率谱的低频成分和高频成分可分别反映交感神经系统与副交感神经系统的活性，低频、高频能量比可作为评价交感神经系统与副交感神经系统均衡性的指标[117]。Chen等[118]提出一种基于组织氧饱和度的非接触式心理压力测量方法，利用采集到的数据建立用于心理压力分类的二分类器，压力状态与平静状态的分类准确率可以达到76.19%。根据达尔文理论[119]，面部表情反映了人体内在的生理反应，当人体处于不同状态时，面部表情会有相应的变化，因此，面部表情可以体现人的心理状态。面部表情与心理压力之间存在密切关系，人的心理压力可通过静态的面部表情预测[120-121]。

在这方面的研究上，孔令琴等[122]提出了一种融合心率变异性HRV与人脸表情的非接触式心理压力检测方法。该方法通过IPPG技术从视频图像中提取HRV信息，并通过VGG19网络建立表情识别模型，获得人脸表情。将HRV及表情共同作为特征输入，利用支持向量机进行训练分类，实现压力状态与非压力状态的检测。该方法能有效提高心理压力检测的准确性，可应用于普通人群、运动员、犯罪人员心理测试等领域。

3.6 心血管疾病监测

脉搏波含有与心血管状态相关的多种生理参数信息，是心血管疾病预防及临床健康监测的重要指标。不同疾病由于其病理原因不同，对血管造成的病变有所不同，使其在脉搏波上的体现也不相同。因此IPPG技术可以用来开展心血管相关疾病的病理分析。

Pilt等[123]采用PPG波形增强指数(PPGAI)估计动脉硬化程度与年龄的关系，采集24名健康受试者和20名2型糖尿病患者的PPG信号，并对PPG信号进行处理与分析。糖尿病患者组与健康受试者相比，其动脉硬化和老化程度有所增加，PPGAI指数可用于糖尿病患者心血管早衰的检测。Schönauer等[124]评估了心脏自主型糖尿病神经病变下的心率变异性特征。年龄、心血管疾病、内皮功能障碍、糖尿病相关微血管动脉硬化以及神经病变对脉搏波特征波形的影响得到了广泛研究[125-127]。

以高血糖为特征的糖尿病是一种几乎影响人体所有动脉血管床的代谢紊乱性疾病[128]，对患者整个血管树产生普遍的血栓性影响，导致大血管动脉粥样硬化和微血管并发症[129]。糖尿病的病程以及程度会不同程度地对血管壁产生损伤，加剧血管缺氧、缺血的程度。血管长期处于循环不畅的状态，其脉搏波波形就产生了巨大变化[130-132]。对于复杂生理参数的检测来说，需要分析不同疾病的病理机理对于血管的影响，从本质上分析出病理在脉搏波上的具体体现，从而选取最佳的监测方式实现心血管健康监测。

针对采用IPPG技术进行心血管疾病生理参数的检测，Xu等[133]开展了针对心脏病房颤类患者以及糖尿病患者的IPPG信号的特征挖掘与疾病分类。图10(a)为房颤类心脏病人RGB通道下的IPPG信号。RGB通道中的IPPG的差分波形是结合多层皮肤组织光学信息和疾病病理机理的综合表现。对于房颤类心脏病人来说，IPPG信号具备单峰、双峰以及三峰的特征。另外，还可以看出，RGB三个通道的峰值特征是十分相似的。对于房颤类心脏病人来说，由于心脏受损而引起的IPPG波形在RGB通道中的特征都是相似的。虽然B通道只到达皮肤组织的表层，但B通

道的IPPG信号也与其他两个通道一样携带着心跳受损的病理特征。图10(b)为糖尿病患者的RGB通道下的IPPG信号。对于患有糖尿病长达2~4年的人来说,IPPG信号在RGB三个通道下的峰值特征存在明显差异,呈现多峰特征,并且峰难以区分。对于糖尿病受试者,高血糖对每层皮肤组织的具体影响明显不一致,很难概括每个糖尿病患者RGB通道IPPG波形的特征。由于R通道的IPPG信号穿透皮肤组织的深度最深,承载着最丰富的皮肤组织生理病理信息。因此,R通道的IPPG波形具有更明显的峰特征。根据不同疾病类型的特点,选择合适的IPPG信号通道作为疾病分类通道,可以提高受试者的分类准确率。

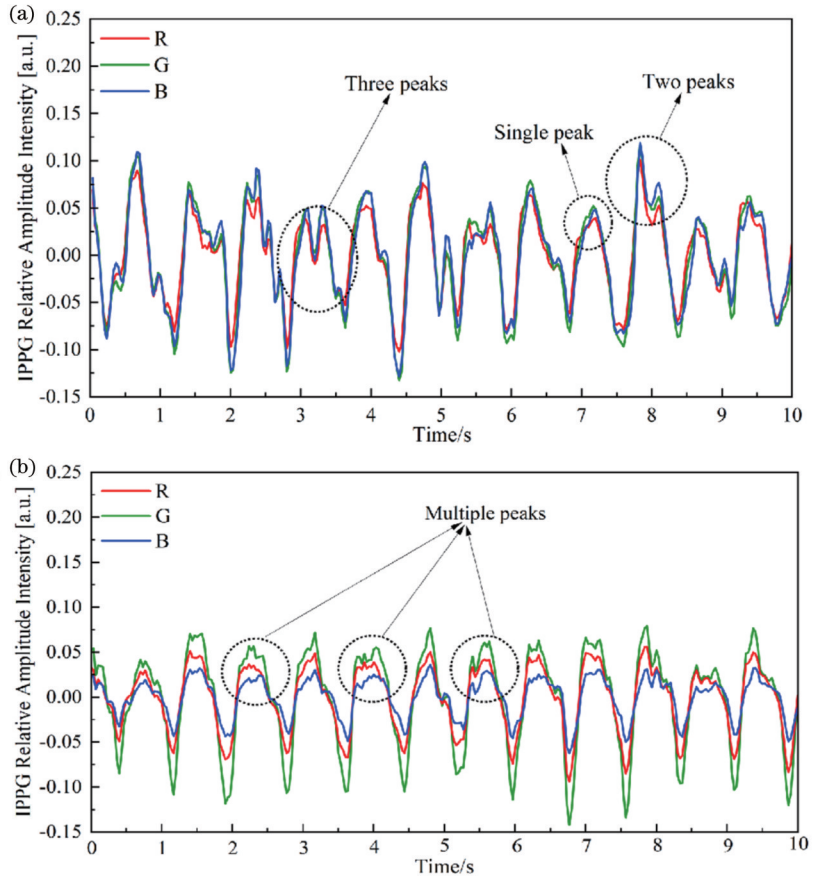

图 10 不同疾病患者的IPPG信号波形特征[133]。(a)房颤类心脏病患者的IPPG信号特征;(b)糖尿病患者的IPPG信号特征

Fig. 10 IPPG signal waveform characteristics of patients with different diseases[133]. (a) IPPG signal characteristics in patients with atrial fibrillation related heart disease; (b) IPPG signal characteristics in patients with diabetes mellitus

4 IPPG技术展望

IPPG技术能够获取从人体循环系统到呼吸系统的大量病理与生理信息,是对心率、心率变异性以及血氧饱和度等基础生理参数进行远程、连续以及无创检测的重要手段。随着对IPPG技术研究的不断深入,IPPG技术应用于动脉疾病、僵硬以及衰老等复杂心血管生理参数的监测与评估得到了高度认可。IPPG技术对于心血管疾病的日常健康监测上也显示出了巨大潜力,有望成为辅助医疗疾病诊断的重要工具。

除了医疗方面的重要应用,IPPG技术在日常生活方面也具有广泛的应用前景。IPPG技术可以通过检测由于血液容积变化引起的皮肤组织漫反射光强的变化获得脉搏波等人体生理信息,因此其可用于活体皮肤识别,进而用于人脸防伪。这使其有望广泛应用于机场安检、地铁安检以及在线支付中,避免采用伪装人脸进行欺骗的行为。此外,鉴于IPPG技术的活体皮肤检测能力,将其搭载于无人机或救援机器人的摄像系统中,可用于协助在事故、灾难现场中对幸存者的救援行动。IPPG技术还可通过获取的生理参数及表情信息来分析受试者的情绪和心理状态,并用于分析受试者在游戏中的认知压力与情绪变化。因此该技术未来有望用于娱乐场景如虚拟现实、增强现实以及人机交互的游戏设备中检测使用者的情绪反应。此外,该技术有望开发成非接触式隐藏测谎仪,用于对审讯过程中犯罪嫌疑人或恐怖分子的心理压力评估。

5 结束语

IPPG技术具备非接触、性价比高、设备操作简单、

能够对受试者进行连续自动生理参数监测等优点，在生物医学研究、临床医学、日常生活身体健康状况监测中具有重要的研究意义和应用价值。随着光学成像器件及成像技术的发展，IPPG技术逐渐向小型化、智能化方向发展，其监测指标以及监测精度等也在不断提高。IPPG技术定量分析在体组织光学特性及生理病理变化特征，提高在体成分定量检测精度，这对于拓展IPPG技术的临床应用具有十分重要的意义。IPPG技术是一种典型的多维图像数据，与深度学习技术相结合，进一步对获取的人体生理参数信息进行评估，是深入理解生物组织的光学特性和探究复杂心血管疾病相关病理机理的重要手段。在疾病早期诊断、个体精准医疗以及日常生活情绪监测等具有十分良好的应用前景。

参 考 文 献

[1] Loukogeorgakis S, Dawson R, Phillips N, et al. Validation of a device to measure arterial pulse wave velocity by a photoplethysmographic method[J]. Physiological Measurement, 2002, 23(3): 581-596.

[2] Hertzman A B, Spealman C R. Observation on the finger volume pulse recorded photoelectrically[J]. The American Journal of Physiology, 1937, 119: 334-335.

[3] Hertzman A B. The blood supply of various skin areas as estimated by the photoelectric plethysmograph[J]. American Journal of Physiology-Legacy Content, 1938, 124(2): 328-340.

[4] Sanyal S, Nundy K K. Algorithms for monitoring heart rate and respiratory rate from the video of a user's face[J]. IEEE Journal of Translational Engineering in Health and Medicine, 2018, 6: 2700111.

[5] Poh M Z, McDuff D J, Picard R W. Non-contact, automated cardiac pulse measurements using video imaging and blind source separation[J]. Optics Express, 2010, 18(10): 10762-10774.

[6] Prathosh A P, Praveena P, Mestha L K, et al. Estimation of respiratory pattern from video using selective ensemble aggregation[J]. IEEE Transactions on Signal Processing, 2017, 65(11): 2902-2916.

[7] Rasche S, Trumpp A, Waldow T, et al. Camera-based photoplethysmography in critical care patients[J]. Clinical Hemorheology and Microcirculation, 2016, 64(1): 77-90.

[8] Soleimani V, Mirmehdi M, Damen D M, et al. Depth-based whole body photoplethysmography in remote pulmonary function testing[J]. IEEE Transactions on Biomedical Engineering, 2017, 65(6): 1421-1431.

[9] Allen J. Photoplethysmography and its application in clinical physiological measurement[J]. Physiological Measurement, 2007, 28(3): R1-R39.

[10] Bortolotto L A, Blacher J, Kondo T, et al. Assessment of vascular aging and atherosclerosis in hypertensive subjects: second derivative of photoplethysmogram versus pulse wave velocity[J]. American Journal of Hypertension, 2000, 13(2): 165-171.

[11] Miyai N, Miyashita K, Arita M, et al. Noninvasive assessment of arterial distensibility in adolescents using the second derivative of photoplethysmogram waveform[J]. European Journal of Applied Physiology, 2001, 86(2): 119-124.

[12] Verkruysse W, Svaasand L O, Nelson J S. Remote plethysmographic imaging using ambient light[J]. Optics Express, 2008, 16(26): 21434-21445.

[13] Kamshilin A A, Margaryants N B. Origin of photoplethysmographic waveform at green light[J]. Physics Procedia, 2017, 86: 72-80.

[14] Kamshilin A A, Nippolainen E, Sidorov I S, et al. A new look at the essence of the imaging photoplethysmography[J]. Scientific Reports, 2015, 5: 10494.

[15] Kwon S, Kim J, Lee D, et al. ROI analysis for remote photoplethysmography on facial video[C]//2015 37th Annual International Conference of the IEEE Engineering in Medicine and Biology Society (EMBC), August 25-29, 2015, Milan, Italy. New York: IEEE Press, 2015: 4938-4941.

[16] Alian A A, Shelley K H. Photoplethysmography[J]. Best Practice & Research Clinical Anaesthesiology, 2014, 28(4): 395-406.

[17] Sun Y, Azorin-Peris V, Kalawsky R, et al. Use of ambient light in remote photoplethysmographic systems: comparison between a high-performance camera and a low-cost webcam[J]. Journal of Biomedical Optics, 2012, 17(3): 037005.

[18] Hanzlik P J, Deeds F, Terada B. A simple method of demonstrating changes in blood supply of the ear and effects of some measures[J]. Journal of Pharmacology and Experimental Therapeutics, 1936, 56(2): 194-204.

[19] Reisner A, Shaltis P A, McCombie D, et al. Utility of the photoplethysmogram in circulatory monitoring[J]. Anesthesiology, 2008, 108(5): 950-958.

[20] Wang W. Robust and automatic remote photoplethysmography [D]. The Netherlands: Technische Universiteit Eindhoven, 2017.

[21] Volkov M V, Margaryants N B, Potemkin A V, et al. Video capillaroscopy clarifies mechanism of the photoplethysmographic waveform appearance[J]. Scientific Reports, 2017, 7: 13298.

[22] Nitzan M, Adar Y, Hoffman E, et al. Comparison of systolic blood pressure values obtained by photoplethysmography and by Korotkoff sounds[J]. Sensors, 2013, 13(11): 14797-14812.

[23] Daly S M, Leahy M J. '*Go with the flow*': a review of methods and advancements in blood flow imaging[J]. Journal of Biophotonics, 2013, 6(3): 217-255.

[24] Teplov V, Nippolainen E, Makarenko A A, et al. Ambiguity of mapping the relative phase of blood pulsations[J]. Biomedical Optics Express, 2014, 5(9): 3123-3139.

[25] Sidorov I S, Romashko R V, Koval V T, et al. Origin of infrared light modulation in reflectance-mode photoplethysmography[J]. PLoS One, 2016, 11(10): e0165413.

[26] Dong A Y, Honnorat N, Gaonkar B, et al. CHIMERA: clustering of heterogeneous disease effects via distribution matching of imaging patterns[J]. IEEE Transactions on Medical Imaging, 2016, 35(2): 612-621.

[27] Varol E, Sotiras A, Davatzikos C. HYDRA: revealing heterogeneity of imaging and genetic patterns through a multiple max-margin discriminative analysis framework[J]. NeuroImage, 2017, 145: 346-364.

[28] Viola P, Jones M. Rapid object detection using a boosted cascade of simple features[C]//Proceedings of the 2001 IEEE Computer Society Conference on Computer Vision and Pattern Recognition. CVPR, December 8-14, 2001, Kauai, HI, USA. New York: IEEE Press, 2003.

[29] Baltrusaitis T, Robinson P, Morency L P. Constrained local neural fields for robust facial landmark detection in the wild[C]// 2013 IEEE International Conference on Computer Vision Workshops, December 2-8, 2013, Sydney, NSW, Australia. New York: IEEE Press, 2014: 354-361.

[30] Baltrušaitis T, Robinson P, Morency L P. 3D constrained local model for rigid and non-rigid facial tracking[C]//2012 IEEE Conference on Computer Vision and Pattern Recognition, June 16-21, 2012, Providence, RI, USA. New York: IEEE Press, 2012: 2610-2617.

[31] Henriques J F, Caseiro R, Martins P, et al. Exploiting the circulant structure of tracking-by-detection with kernels[M]//

Fitzgibbon A, Lazebnik S, Perona P, et al. Computer vision-ECCV 2012. Lecture notes in computer science. Heidelberg: Springer, 2012, 7575: 702-715.

[32] Li X B, Chen J, Zhao G Y, et al. Remote heart rate measurement from face videos under realistic situations[C]// 2014 IEEE Conference on Computer Vision and Pattern Recognition, June 23-28, 2014, Columbus, OH, USA. New York: IEEE Press, 2014: 4264-4271.

[33] 刘蕾, 董洪伟, 童晶. 基于视频的心率测量算法研究[J]. 计算机工程与应用, 2015, 51(18): 199-203.
Liu L, Dong H W, Tong J. Video-based heart rate measuring method[J]. Computer Engineering and Applications, 2015, 51(18): 199-203.

[34] Bal U. Non-contact estimation of heart rate and oxygen saturation using ambient light[J]. Biomedical Optics Express, 2015, 6(1): 86-97.

[35] Wang W J, Stuijk S, de Haan G. Unsupervised subject detection via remote PPG[J]. IEEE Transactions on Biomedical Engineering, 2015, 62(11): 2629-2637.

[36] Wang W J, Stuijk S, de Haan G. Living-skin classification via remote-PPG[J]. IEEE Transactions on Biomedical Engineering, 2017, 64(12): 2781-2792.

[37] Liu H, Chen T, Zhang Q N, et al. A new approach for face detection based on photoplethysmographic imaging[M]//Yin X X, Ho K, Zeng D, et al. Health information science. Lecture notes in computer science. Cham: Springer, 2015, 9085: 79-91.

[38] Tarassenko L, Villarroel M, Guazzi A, et al. Non-contact video-based vital sign monitoring using ambient light and auto-regressive models[J]. Physiological Measurement, 2014, 35(5): 807-831.

[39] 林岚, 张柏雯, 王婧璇, 等. 认知储备在大脑老化中的研究进展[J]. 医疗卫生装备, 2017, 38(9): 93-98.
Lin L, Zhang B W, Wang J X, et al. Research advance of cognitive reserve in brain aging[J]. Chinese Medical Equipment Journal, 2017, 38(9): 93-98.

[40] Budd Haeberlein S, O'Gorman J, Chiao P, et al. Clinical development of aducanumab, an anti-aβ human monoclonal antibody being investigated for the treatment of early Alzheimer's disease[J]. The Journal of Prevention of Alzheimer's Disease, 2017, 4(4): 255-263.

[41] Poh M Z, McDuff D J, Picard R W. Advancements in noncontact, multiparameter physiological measurements using a webcam[J]. IEEE Transactions on Biomedical Engineering, 2011, 58(1): 7-11.

[42] Lewandowska M, Rumiński J, Kocejko T, et al. Measuring pulse rate with a webcam: a non-contact method for evaluating cardiac activity[C]//2011 Federated Conference on Computer Science and Information Systems (FedCSIS), September 18-21, 2011, Szczecin, Poland. New York: IEEE Press, 2011: 405-410.

[43] Wang W J, Stuijk S, de Haan G. A novel algorithm for remote photoplethysmography: spatial subspace rotation[J]. IEEE Transactions on Biomedical Engineering, 2016, 63(9): 1974-1984.

[44] Wang W J, den Brinker A C, Stuijk S, et al. Algorithmic principles of remote PPG[J]. IEEE Transactions on Bio-Medical Engineering, 2017, 64(7): 1479-1491.

[45] Lee H, Ko H, Chung H, et al. Robot assisted instantaneous heart rate estimator using camera based remote photoplethysmograpy via plane-orthogonal-to-skin and finite state machine[C]//2020 42nd Annual International Conference of the IEEE Engineering in Medicine & Biology Society (EMBC), July 20-24, 2020, Montreal, QC, Canada. New York: IEEE Press, 2020: 4425-4428.

[46] De Haan G, Jeanne V. Robust pulse rate from chrominance-based rPPG[J]. IEEE Transactions on Biomedical Engineering, 2013, 60(10): 2878-2886.

[47] de Haan G, van Leest A. Improved motion robustness of remote-PPG by using the blood volume pulse signature[J]. Physiological Measurement, 2014, 35(9): 1913-1926.

[48] Unakafov A M, Möller S, Kagan I, et al. Using imaging photoplethysmography for heart rate estimation in non-human Primates[J]. PLoS One, 2018, 13(8): e0202581.

[49] Wang W J, den Brinker A C, Stuijk S, et al. Robust heart rate from fitness videos[J]. Physiological Measurement, 2017, 38(6): 1023-1044.

[50] Wang W J, den Brinker A C, Stuijk S, et al. Color-distortion filtering for remote photoplethysmography[C]//2017 12th IEEE International Conference on Automatic Face & Gesture Recognition (FG 2017), May 30-June 3, 2017, Washington, DC, USA. New York: IEEE Press, 2017: 71-78.

[51] Zhang F, Chen S X, Zhang H S, et al. Bioelectric signal detrending using smoothness prior approach[J]. Medical Engineering & Physics, 2014, 36(8): 1007-1013.

[52] Bousefsaf F, Maaoui C, Pruski A. Continuous wavelet filtering on webcam photoplethysmographic signals to remotely assess the instantaneous heart rate[J]. Biomedical Signal Processing and Control, 2013, 8(6): 568-574.

[53] Holton B D, Mannapperuma K, Lesniewski P J, et al. Signal recovery in imaging photoplethysmography[J]. Physiological Measurement, 2013, 34(11): 1499-1511.

[54] Favilla R, Zuccalà V C, Coppini G. Heart rate and heart rate variability from single-channel video and ICA integration of multiple signals[J]. IEEE Journal of Biomedical and Health Informatics, 2019, 23(6): 2398-2408.

[55] Siddiqui S A, Zhang Y, Feng Z Q, et al. A pulse rate estimation algorithm using PPG and smartphone camera[J]. Journal of Medical Systems, 2016, 40(5): 126.

[56] Amelard R, Clausi D A, Wong A. Spectral-spatial fusion model for robust blood pulse waveform extraction in photoplethysmographic imaging[J]. Biomedical Optics Express, 2016, 7(12): 4874-4885.

[57] Laure D, Paramonov I. Improved algorithm for heart rate measurement using mobile phone camera[C]//2013 13th Conference of Open Innovations Association (FRUCT), April 22-26, 2013, Petrozavodsk. New York: IEEE Press, 2013: 85-93.

[58] Yu Y P, Raveendran P, Lim C L. Heart rate estimation from facial images using filter bank[C]//2014 6th International Symposium on Communications, Control and Signal Processing (ISCCSP), May 21-23, 2014, Athens, Greece. New York: IEEE Press, 2014: 69-72.

[59] Kumar M, Veeraraghavan A, Sabharwal A. DistancePPG: robust non-contact vital signs monitoring using a camera[J]. Biomedical Optics Express, 2015, 6(5): 1565-1588.

[60] Wang D L, Yang X Z, Liu X N, et al. Detail-preserving pulse wave extraction from facial videos using consumer-level camera [J]. Biomedical Optics Express, 2020, 11(4): 1876-1891.

[61] Villarroel M, Guazzi A, Jorge J, et al. Continuous non-contact vital sign monitoring in neonatal intensive care unit[J]. Healthcare Technology Letters, 2014, 1(3): 87-91.

[62] Jayadevappa B M, Holi M. An estimation technique using FFT for heart rate derived from PPG signal[J]. Global Journals of Research in Engineering, 2015, 15(F7): 45-51.

[63] Kong L Q, Wu Y H, Zhao Y J, et al. Robust imaging photoplethysmography in long-distance motion[J]. IEEE Photonics Journal, 2020, 12(3): 3900512.

[64] Chen D S, Liu Z K. A survey of skin color detection[J]. Chinese Journal of Computers, 2006, 29(2): 194-207.

[65] 程超, 达飞鹏, 王辰星, 等. 基于Lucas-Kanade算法的最大Gabor相似度大姿态人脸识别[J]. 光学学报, 2019, 39(7): 0715005.
Cheng C, Da F P, Wang C X, et al. Pose invariant face recognition using maximum Gabor similarity based on Lucas-

Kanade algorithm[J]. Acta Optica Sinica, 2019, 39(7): 0715005.
[66] 孟濬, 赵夕朦. 基于皮肤表面“振动信号”的多摄像头人体识别定位[J]. 光学学报, 2019, 39(5): 0515001.
Meng J, Zhao X M. Human body recognition and positioning with multiple cameras based on “vibration signals” from skin surfaces[J]. Acta Optica Sinica, 2019, 39(5): 0515001.
[67] Gibert G, D′Alessandro D, Lance F. Face detection method based on photoplethysmography[C]//2013 10th IEEE International Conference on Advanced Video and Signal Based Surveillance, August 27-30, 2013, Krakow, Poland. New York: IEEE Press, 2013: 449-453.
[68] Ren X, Malik J. Learning a classification model for segmentation [C]//Proceedings Ninth IEEE International Conference on Computer Vision, October 13-16, 2003, Nice, France. New York: IEEE Press, 2008: 10-17.
[69] Mori G. Guiding model search using segmentation[C]//Tenth IEEE International Conference on Computer Vision (ICCV′05) Volume 1, October 17-21, 2005, Beijing, China. New York: IEEE Press, 2005: 1417-1423.
[70] Levinshtein A, Stere A, Kutulakos K N, et al. TurboPixels: fast superpixels using geometric flows[J]. IEEE Transactions on Pattern Analysis and Machine Intelligence, 2009, 31(12): 2290-2297.
[71] Vedaldi A, Soatto S. Quick shift and kernel methods for mode seeking[M]//Forsyth D, Torr P, Zisserman Z. Computer vision-ECCV 2008. Lecture notes in computer science. Heidelberg: Springer, 2008, 5305: 705-718.
[72] Achanta R, Shaji A, Smith K, et al. SLIC superpixels[J]. EPFL Technical Report, 2010: 149300.
[73] Achanta R, Shaji A, Smith K, et al. SLIC superpixels compared to state-of-the-art superpixel methods[J]. IEEE Transactions on Pattern Analysis and Machine Intelligence, 2012, 34(11): 2274-2282.
[74] 孔令琴, 吴育恒, 赵跃进, 等. 基于超像素分割的IPPG活体皮肤检测[J]. 光学学报, 2020, 40(13): 1310001.
Kong L Q, Wu Y H, Zhao Y J, et al. IPPG alive-skin detection based on superpixel segmentation[J]. Acta Optica Sinica, 2020, 40(13): 1310001.
[75] 尹聪, 李文秀. 光电脉搏仪在血氧饱和度测量中的应用[J]. 无线互联科技, 2022, 19(15): 106-108.
Yin C, Li W X. Application of photoelectric pulse meter in blood oxygen saturation measurement[J]. Wireless Internet Technology, 2022, 19(15): 106-108.
[76] Haacke E M, Lai S, Reichenbach J R, et al. *In vivo* measurement of blood oxygen saturation using magnetic resonance imaging: a direct validation of the blood oxygen level-dependent concept in functional brain imaging[J]. Human Brain Mapping, 1997, 5(5): 341-346.
[77] Shao D D, Liu C B, Tsow F, et al. Noncontact monitoring of blood oxygen saturation using camera and dual-wavelength imaging system[J]. IEEE Transactions on Biomedical Engineering, 2016, 63(6): 1091-1098.
[78] Humphreys K, Ward T, Markham C. Noncontact simultaneous dual wavelength photoplethysmography: a further step toward noncontact pulse oximetry[J]. Review of Scientific Instruments, 2007, 78(4): 044304.
[79] Fei J, Pavlidis I. Thermistor at a distance: unobtrusive measurement of breathing[J]. IEEE Transactions on Biomedical Engineering, 2010, 57(4): 988-998.
[80] Gioux S, Stockdale A, Oketokoun R, et al. First-in-human pilot study of a spatial frequency domain oxygenation imaging system[J]. Journal of Biomedical Optics, 2011, 16(8): 086015.
[81] Humphreys K, Ward T, Markham C. A CMOS camera-based pulse oximetry imaging system[C]//2005 IEEE Engineering in Medicine and Biology 27th Annual Conference, January 17-18, 2006, Shanghai, China. New York: IEEE Press, 2006: 3494-3497.
[82] Guazzi A R, Villarroel M, Jorge J, et al. Non-contact measurement of oxygen saturation with an RGB camera[J]. Biomedical Optics Express, 2015, 6(9): 3320-3338.
[83] Tsai H Y, Huang K C, Chang H C, et al. A noncontact skin oxygen-saturation imaging system for measuring human tissue oxygen saturation[J]. IEEE Transactions on Instrumentation and Measurement, 2014, 63(11): 2620-2631.
[84] Harford M, Catherall J, Gerry S, et al. Availability and performance of image-based, non-contact methods of monitoring heart rate, blood pressure, respiratory rate, and oxygen saturation: a systematic review[J]. Physiological measurement, 2019, 40(6): 06TR01.
[85] Wieringa F P, Mastik F, van der Steen A F W. Contactless multiple wavelength photoplethysmographic imaging: a first step toward “SpO_2 camera” technology[J]. Annals of Biomedical Engineering, 2005, 33(8): 1034-1041.
[86] Wieringa F P, Mastik F, Boks R H, et al. *In vitro* demonstration of an SpO_2^- camera[C]//2007 Computers in Cardiology, September 30-October 3, 2007, Durham, NC, USA. New York: IEEE Press, 2009: 749-751.
[87] Al-Naji A, Khalid G A, Mahdi J F, et al. Non-contact SpO_2 prediction system based on a digital camera[J]. Applied Sciences, 2021, 11(9): 4255.
[88] Li J, Dunmire B, Beach K W, et al. A reflectance model for non-contact mapping of venous oxygen saturation using a CCD camera[J]. Optics Communications, 2013, 308: 78-84.
[89] Kong L Q, Zhao Y J, Dong L Q, et al. Non-contact detection of oxygen saturation based on visible light imaging device using ambient light[J]. Optics Express, 2013, 21(15): 17464-17471.
[90] Leung A. Multimedia, communication and computing application [M]. Boston: CRC Press, 2015: 526.
[91] Fu R R, Wang H. Detection of driving fatigue by using noncontact EMG and ECG signals measurement system[J]. International Journal of Neural Systems, 2014, 24(3): 1450006.
[92] Miyajima C, Nishiwaki Y, Ozawa K, et al. Driver modeling based on driving behavior and its evaluation in driver identification[J]. Proceedings of the IEEE, 2007, 95(2): 427-437.
[93] Pilutti T, Ulsoy G. On-line identification of driver state for lane-keeping tasks[C]//Proceedings of 1995 American Control Conference - ACC′95, June 21-23, 1995, Seattle, WA, USA. New York: IEEE Press, 2002: 678-681.
[94] 张希波, 成波, 冯睿嘉. 基于方向盘操作的驾驶人疲劳状态实时检测方法[J]. 清华大学学报(自然科学版), 2010, 50(7): 1072-1076, 1081.
Zhang X B, Cheng B, Feng R J. Real-time detection of driver drowsiness based on steering performance[J]. Journal of Tsinghua University (Science and Technology), 2010, 50(7): 1072-1076, 1081.
[95] Grace R, Byrne V E, Bierman D M, et al. A drowsy driver detection system for heavy vehicles[C]//17th DASC. AIAA/IEEE/SAE. Digital Avionics Systems Conference. (CatProceedings. No. 98CH36267), October 31-November 7, 1998, Bellevue, WA, USA. New York: IEEE Press, 2002: I36/1-I36/8.
[96] Choi I H, Kim Y G. Head pose and gaze direction tracking for detecting a drowsy driver[C]//2014 International Conference on Big Data and Smart Computing (BIGCOMP), January 15-17, 2014, Bangkok. New York: IEEE Press, 2014: 241-244.
[97] Wang H L, Liu H H, Song Z M. Fatigue driving detection system design based on driving behavior[C]//2010 International Conference on Optoelectronics and Image Processing, November 11-12, 2010, Haikou, China. New York: IEEE Press, 2011: 549-552.
[98] Abtahi S, Hariri B, Shirmohammadi S. Driver drowsiness monitoring based on yawning detection[C]//2011 IEEE International Instrumentation and Measurement Technology Conference, May 10-12, 2011, Hangzhou, China. New York:

IEEE Press, 2011.
[99] Putta R, Shinde G N, Lohani P. Real time drowsiness detection system using viola Jones algorithm[J]. International Journal of Computer Applications, 2014, 95(8): 28-34.
[100] Lu Y F, Wang Z C. Detecting driver yawning in successive images[C]//2007 1st International Conference on Bioinformatics and Biomedical Engineering, July 6-8, 2007, Wuhan, China. New York: IEEE Press, 2007: 581-583.
[101] Sabet M, Zoroofi R A, Sadeghniiat-Haghighi K, et al. A new system for driver drowsiness and distraction detection[C]//20th Iranian Conference on Electrical Engineering (ICEE2012), May 15-17, 2012, Tehran, Iran. New York: IEEE Press, 2012: 1247-1251.
[102] Baharav A, Kotagal S, Gibbons V, et al. Fluctuations in autonomic nervous activity during sleep displayed by power spectrum analysis of heart rate variability[J]. Neurology, 1995, 45(6): 1183-1187.
[103] Furman G D, Baharav A, Cahan C, et al. Early detection of falling asleep at the wheel: a Heart Rate Variability approach [C]//2008 Computers in Cardiology, September 14-17, 2008, Bologna, Italy. New York: IEEE Press, 2009: 1109-1112.
[104] Li G, Chung W Y. Detection of driver drowsiness using wavelet analysis of heart rate variability and a support vector machine classifier[J]. Sensors, 2013, 13(12): 16494-16511.
[105] Roman B, Pavel S, Miroslav P, et al. Fatigue indicators of drowsy drivers based on analysis of physiological signals[M]// Crespo J, Maojo V, Martin F, et al. Medical data analysis. Lecture notes in computer science. Heidelberg: Springer, 2001, 2199: 62-68.
[106] Sahayadhas A, Sundaraj K, Murugappan M. Detecting driver drowsiness based on sensors: a review[J]. Sensors, 2012, 12 (12): 16937-16953.
[107] Abe E, Fujiwara K, Hiraoka T, et al. Development of drowsy driving accident prediction by heart rate variability analysis[C]// Signal and Information Processing Association Annual Summit and Conference (APSIPA), 2014 Asia-Pacific, December 9-12, 2014, Siem Reap, Cambodia. New York: IEEE Press, 2015.
[108] Michail E, Kokonozi A, Chouvarda I, et al. EEG and HRV markers of sleepiness and loss of control during car driving[C]// 2008 30th Annual International Conference of the IEEE Engineering in Medicine and Biology Society, August 20-25, 2008, Vancouver, BC, Canada. New York: IEEE Press, 2008: 2566-2569.
[109] Jung S J, Shin H S, Chung W Y. Driver fatigue and drowsiness monitoring system with embedded electrocardiogram sensor on steering wheel[J]. IET Intelligent Transport Systems, 2014, 8 (1): 43-50.
[110] Shin H S, Jung S J, Kim J J, et al. Real time car driver's condition monitoring system[C]//SENSORS, 2010 IEEE, November 1-4, 2010, Waikoloa, HI, USA. New York: IEEE Press, 2011: 951-954.
[111] Beck A, Steer R, Brown G. Manual for the beck depression inventory-II[J]. Psychological Corporation, 1996, 21(88): 1-9.
[112] Davidson J R, Book S W, Colket J T, et al. Assessment of a new self-rating scale for post-traumatic stress disorder[J]. Psychological Medicine, 1997, 27(1): 153-160.
[113] Lavoie J A A, Douglas K S. The perceived stress scale: evaluating configural, metric and scalar invariance across mental health status and gender[J]. Journal of Psychopathology and Behavioral Assessment, 2012, 34(1): 48-57.
[114] Lee E H. Review of the psychometric evidence of the perceived stress scale[J]. Asian Nursing Research, 2012, 6(4): 121-127.
[115] Zhai J, Barreto A. Stress detection in computer users based on digital signal processing of noninvasive physiological variables [C]//2006 International Conference of the IEEE Engineering in Medicine and Biology Society, August 30-September 3, 2006, New York, NY, USA. New York: IEEE Press, 2016: 1355-1358.
[116] Hernandez J, Morris R R, Picard R W. Call center stress recognition with person-specific models[M]//D' Mello S, Graesser A, Schuller B, et al. Affective computing and intelligent interaction. Lecture notes in computer science. Heidelberg: Springer, 2011, 6974: 125-134.
[117] 陶林. 近20年来国内关于研究生压力的研究综述[J]. 北京科技大学学报(社会科学版), 2020, 36(4): 36-42.
Tao L. The review of research on post-graduate stress in China in the past 20 years[J]. Journal of University of Science and Technology Beijing (Social Sciences Edition), 2020, 36(4): 36-42.
[118] Chen T, Yuen P, Richardson M, et al. Detection of psychological stress using a hyperspectral imaging technique[J]. IEEE Transactions on Affective Computing, 2014, 5(4): 391-405.
[119] Schützwohl A, Reisenzein R. Facial expressions in response to a highly surprising event exceeding the field of vision: a test of Darwin's theory of surprise[J]. Evolution and Human Behavior, 2012, 33(6): 657-664.
[120] Lazarus R S. From psychological stress to the emotions: a history of changing outlooks[J]. Annual Review of Psychology, 1993, 44: 1-22.
[121] Little A C, McPherson J, Dennington L, et al. Accuracy in assessment of self-reported stress and a measure of health from static facial information[J]. Personality and Individual Differences, 2011, 51(6): 693-698.
[122] 孔令琴, 陈飞, 赵跃进, 等. 融合心率变异性与表情的非接触心理压力检测[J]. 光学学报, 2021, 41(3): 0310003.
Kong L Q, Chen F, Zhao Y J, et al. Non-contact psychological stress detection combining heart rate variability and facial expressions[J]. Acta Optica Sinica, 2021, 41(3): 0310003.
[123] Pilt K, Meigas K, Ferenets R, et al. Photoplethysmographic signal waveform index for detection of increased arterial stiffness [J]. Physiological Measurement, 2014, 35(10): 2027-2036.
[124] Schönauer M, Thomas A, Morbach S, et al. Cardiac autonomic diabetic neuropathy[J]. Diabetes and Vascular Disease Research, 2008, 5(4): 336-344.
[125] He X C, Goubran R A, Liu X P. Secondary peak detection of PPG signal for continuous cuffless arterial blood pressure measurement[J]. IEEE Transactions on Instrumentation and Measurement, 2014, 63(6): 1431-1439.
[126] Liu W C, Fang X, Chen Q Q, et al. Reliability analysis of an integrated device of ECG, PPG and pressure pulse wave for cardiovascular disease[J]. Microelectronics Reliability, 2018, 87: 183-187.
[127] Lilia C M, Gerson O S, Alvaro M O, et al. Endothelial dysfunction evaluated using photoplethysmography in patients with type 2 diabetes[J]. Journal of Cardiovascular Diseases & Diagnosis, 2015, 3(5): 1-7.
[128] Gibbons G W, Shaw P M. Diabetic vascular disease: characteristics of vascular disease unique to the diabetic patient [J]. Seminars in Vascular Surgery, 2012, 25(2): 89-92.
[129] Nesto R W, Rutter M K. Impact of the atherosclerotic process in patients with diabetes[J]. Acta Diabetologica, 2002, 39(2): S22-S28.
[130] Weber T, O'Rourke M F, Lassnig E, et al. Pulse waveform characteristics predict cardiovascular events and mortality in patients undergoing coronary angiography[J]. Journal of Hypertension, 2010, 28(4): 797-805.
[131] Avolio A P, Butlin M, Walsh A. Arterial blood pressure measurement and pulse wave analysis: their role in enhancing cardiovascular assessment[J]. Physiological Measurement, 2010, 31(1): R1-R47.
[132] Yokoyama H, Shoji T, Kimoto E, et al. Pulse wave velocity in lower-limb arteries among diabetic patients with peripheral arterial disease[J]. Journal of Atherosclerosis and Thrombosis,

2003, 10(4): 253-258.
[133] Xu G, Dong L Q, Yuan J, et al. Rational selection of RGB channels for disease classification based on IPPG technology[J]. Biomedical Optics Express, 2022, 13(4): 1820-1833.

Non-Contact Physiological Parameter Detection and Its Application Based on Imaging Photoplethysmography

Kong Lingqin[1,2,3], Zhao Yuejin[1,2,3*], Dong Liquan[1,2,3], Liu Ming[1,2,3], Xu Ge[1], Hui Mei[1], Chu Xuhong[1,2,3]

[1]*School of Optics and Photonics, Beijing Institute of Technology, Beijing* 100081, *China*;
[2]*Beijing Key Laboratory for Precision Optoelectronic Measurement Instrument and Technology, Beijing* 100081, *China*;
[3]*Yangtze Delta Region Academy of Beijing Institute of Technology, Jiaxing* 314019, *Zhejiang, China*

Abstract

Significance Imaging photoplethysmography (IPPG) has the advantages of high cost performance, simple equipment operation, and continuous automatic measurement and observation of subjects. IPPG has become an important means to deeply understand the optical properties of biological tissue and explore the pathological mechanisms related to complex cardiovascular diseases. IPPG is developed on the basis of traditional single-point photoplethysmography (PPG). IPPG uses imaging equipment to record the tiny changes in skin colors caused by the diffuse reflected light carrying the pulsation information of the heart after the interaction between light and skin tissue in the form of continuous images. Then, through video and image processing technologies, human vital sign information such as pulse, heart rate, and heart rate variability are extracted from the video stream. IPPG can reveal the dynamic and small changes in biological tissue during physiological and pathological processes. Therefore, IPPG can be used to better understand basic life activities and realize highly sensitive diagnoses and high-precision quantitative characterization of diseases. IPPG is applicable to large-scale clinical detection and physical health monitoring in daily life and other scenarios. It is a research hotspot of human daily physiological status monitoring in the new era of medical health.

Progress In recent years, due to the continuous improvement of imaging sensor resolution and various signal processing technologies, IPPG has made great progress in the detection and application of human physiological parameters, such as heart rate, respiratory rate, and heart rate variability, as well as the application of disease diagnosis, such as arterial disease, stiffness and aging, and chronic microcirculation disease. However, for the further monitoring and classification diagnosis of complex cardiovascular diseases, IPPG still faces the challenges of lack of pathological feature analysis, complex optical feature parameters, and the manifestation of different types of pathological mechanisms of cardiovascular diseases on pulse waves. Therefore, we summarize the basic research and application of the existing IPPG and continue to explore the optical mechanism and pathological mechanism of IPPG. These efforts are very important for guiding the future development of IPPG.

Based on a comprehensive investigation of a large number of relevant literatures on the monitoring of human physiological parameters by IPPG in China and abroad in the past 20 years and our long-term research work, we first introduce the optical principle of IPPG. Then, we analyze the new method of IPPG signals in video image processing and that of improving the signal-to-noise ratio (Table 1), including a series of mainstream methods for selecting imaging sites in different areas of skin tissue and those for motion artifacts and blur. Finally, the clinical application of IPPG is introduced in detail, mainly including the extraction of IPPG heart rate under adaptive focal length, detection of living skin, measurement of blood oxygen saturation under visible light (Fig. 7), monitoring of fatigue status, evaluation of psychological stress, and analysis of the pathological mechanism of IPPG signals under cardiovascular diseases (Fig. 9).

Conclusions and Prospects IPPG is gradually developing towards miniaturization and intelligence. The monitoring indicators and accuracy of IPPG are continuously improving, which has important research significance and application value in biomedical research, clinical medicine, and daily life health monitoring. As an effective tool for early diagnosis of diseases and individual precision medical treatment, IPPG still needs in-depth and detailed exploration to promote its further development in academic and engineering fields.

Key words imaging photoplethysmography; physiological parameter detection; cardiovascular monitoring